Fluid Phase Equilibria 356 (2013) 46–55

Contents lists available at ScienceDirect

Fluid Phase Equilibria

journal homepage: www.elsevier.com/locate/fluid

Cross-diffusion in a colloid–polymer aqueous system

Michele S. McAfee, Onofrio Annunziata*

Contribution from the Department of Chemistry, Texas Christian University, Fort Worth, TX 76129, USA

ARTICLE INFO

Article history:
Received 9 May 2013
Received in revised form 6 July 2013
Accepted 8 July 2013
Available online 17 July 2013

Keywords:
Tyloxapol
Polyethylene glycol
Excluded volume
Hydration
Depletion

ABSTRACT

The thermodynamic behavior of colloid–polymer systems has been extensively investigated. However, relatively few studies have been reported on the corresponding transport properties. We have measured the four multicomponent diffusion coefficients for a ternary colloid–polymer-water system by Rayleigh interferometry at 25 °C. The colloidal particles and polymer coils in our system are the tyloxapol micelles and polyethylene glycol (molecular weight of 2.0 kg mol^{-1}) respectively. Both solutes are neutral and preferentially interact with water. Our investigation focused on the behavior of the two cross-diffusion coefficients in dilute solutions. These coefficients characterize how the concentration gradient of colloidal particles (polymer coils) affects the diffusion rate of polymer coils (colloidal particles). Our data were used to extract two fundamental parameters describing the thermodynamic and kinetic factors responsible for cross-diffusion. The comparison of our experimental results with a proposed reference model based on the hydrodynamic volume of particles indicates that excluded-volume thermodynamic interactions and solute hydration represent the main contributions to cross-diffusion coefficients. The role of the aggregation number of micelles and the effect of polydispersity on cross-diffusion parameters were also examined.

1. Introduction

Multicomponent systems containing nanoparticles, surfactants, polymers and other macromolecules in solution have attracted much attention due to their important role in industrial applications and biological functions. For example, understanding the interaction between polymers and colloidal particles is important for colloid stabilization and destabilization, flocculation, coating, biotechnology, and detergency [1–3].

For ternary colloid–polymer–solvent mixtures, it is generally believed that the main mechanism of action of polymer coils on colloidal particles can be described through the influence of mutual volume exclusion on the entropy of the system. This mechanism is usually denoted using the terms: "depletion" or "excluded-volume" interaction. Related models have been successful in describing the effect of polymers on model colloidal suspensions especially in relation to their phase transitions [4–7].

Excluded-volume interactions lead to thermodynamic non-ideality in colloid–polymer–solvent systems. Due to steric hindrance, the center of mass of a polymer coil is not only excluded from the volume occupied by the colloidal particles but also from a region surrounding them denoted as the depletion layer. The width of this layer is proportional to the size of the polymer coil. Thus, the effective concentration of a polymer coil, i.e. the concentration of polymer in the free volume, is significantly higher than its actual concentration [6,7].

Excluded-volume interactions are also expected to be important in living systems. Indeed, the total concentration of macromolecules inside cell is very high, in the range of 300–400 g/L. Thus, the effective concentration of each macromolecular species is significantly greater than its actual concentration. This difference has kinetic and thermodynamic consequences on the conformational stability, aggregation behavior and biological functions of that macromolecule. The effect of excluded-volume interactions on the biophysical behavior of biological macromolecules is usually denoted as "macromolecular crowding" [8,9].

Most investigations on colloid–polymer–solvent systems have focused on the thermodynamic properties of macromolecular systems and their consequences on phase transitions [6,7,10–12]. However, relatively few studies have been reported on transport properties such as diffusion. Diffusion is important for applications in which concentration gradients occur such as controlled-release technologies [13,14], separation science [15] and microfluidics [16,17]. It is also an important kinetic parameter for phase transitions [18,19], reaction kinetics [20,21] and dynamics of living systems [22–24]. Therefore, diffusion studies on multicomponent systems containing colloidal particles and macromolecules are needed.

There are diffusion studies that have focused on understanding how macromolecular crowding affects the Brownian mobility of

* Corresponding author. Tel.: +1 817 257 6215; fax: +1 817 257 5851.
E-mail address: O.Annunziata@tcu.edu (O. Annunziata).

0378-3812/$ – see front matter © 2013 Elsevier B.V. All rights reserved.
http://dx.doi.org/10.1016/j.fluid.2013.07.014

macromolecules [25,26]. However, this aspect represents only one effect of excluded-volume interactions on the diffusion processes. Another important aspect of diffusion processes is cross-diffusion, and appears in multicomponent systems, i.e. those systems containing at least two solute components [27]. In the specific case of a ternary solute(1)–solute(2)–solvent system, cross-diffusion can be introduced through the extended Fick's first law [28]:

$$-J_1 = D_{11}\nabla C_1 + D_{12}\nabla C_2 \tag{1a}$$

$$-J_2 = D_{21}\nabla C_1 + D_{22}\nabla C_2 \tag{1b}$$

where C_1 and C_2 are the molar concentrations of the two solutes, J_1 and J_2 are the corresponding fluxes and the four D_{ij}'s (with $i, j = 1, 2$) are the multicomponent diffusion coefficients. Main-diffusion coefficients, D_{11} and D_{22}, describe the flux of a solute due to its own concentration gradient, and they are approximately related to the Brownian mobility of solute particles. The cross-diffusion coefficients, D_{12} and D_{21}, describe the flux of a solute due to the concentration gradient of the other solute. While main-diffusion coefficients are normally positive, cross-diffusion coefficients can be either positive or negative depending on solute(1)–solute(2) net interactions.

Understanding multicomponent diffusion is important for colloid(1)–polymer(2)–solvent mixtures. For example, we can already appreciate that a concentration gradient of colloidal particles, ∇C_1, in the presence of a uniform concentration of polymer coils, $\nabla C_2 = 0$, will generate a gradient of effective concentration of polymer coils in the same direction due to excluded-volume effects. Thus, it can be deduced that ∇C_1 can induce cross-diffusion of polymer coils from high to low C_1 ($D_{21} > 0$). Clearly, the mechanism of cross-diffusion should depend on excluded-volume interactions.

There are experimental and theoretical studies that have examined the effect of excluded-volume interactions on cross-diffusion in protein-polymer and polymer-polymer aqueous systems [29–31]. However, proposed excluded-volume models satisfactorily describe the experimental behavior of one of the two cross-diffusion coefficients only. One limitation of proposed models is the assumption that the mechanism cross-diffusion is a consequence of thermodynamic non-ideality and factors not related to equilibrium properties were neglected. A few other diffusion studies on multicomponent diffusion of macromolecular systems have not addressed the role of excluded-volume interactions [32,33].

In this paper, we report an experimental investigation of multicomponent diffusion for a ternary colloid–polymer–water system in isothermal conditions. Specifically, we choose tyloxapol micelles as colloidal particles (1) and polyethylene glycol with molecular weight of 2.0 kg mol^{-1} (PEG) as polymer coils (2) PEG is a hydrophilic nonionic polymer utilized in many biochemical and pharmaceutical applications. Due to its mild action on the biological activity of cell components, PEG is commonly used for liquid–liquid partitioning, the precipitation of biomacromolecules and the preparation of biomaterials [34–36]. It is generally believed that the main mechanism of action of PEG on globular macromolecules can be described through the mechanism of excluded-volume interactions [37–39]. Moreover, PEG is also employed to mimic the crowded environment inside living cells [40,41].

Tyloxapol is a nonionic surfactant mostly used in marketed ophthalmic products and as a mucolytic agent for treating pulmonary diseases, and is essentially an oligomer of octoxynol 9 (Triton X-100) [42,43]. Tyloxapol has a critical micellar concentration (cmc) of 0.0385 g/L in water at 25 °C [42]. This cmc value is much lower than that of Triton X-100. Hence, the presence of free surfactant can be neglected with respect to micellar surfactant even in fairly dilute solutions. Tyloxapol micelles are spherical with a diameter of 7 nm, and their size and shape do not change significantly for concentration as high as 10% by weight according to cryo-transmission electron microscopy [43]. The hydrophilic groups on the surface of tyloxapol micelles are poly(ethylene) glycol chains. Thus, the chemical nature of the micelle surface is the same as that of the other solute component. Moreover, polymer adsorption on the micelle surface is not expected to occur due to the preferential interaction of the ethoxy group with water.

We measured the four multicomponent diffusion coefficients, $D_{ij}(C_1,C_2)$, in dilute solutions at 25 °C by Rayleigh interferometry [44,45]. We show how these diffusion coefficients can be used to extract two fundamental quantities responsible for cross-diffusion. These are a thermodynamic non-ideality parameter, which can be related to equilibrium excluded-volume interactions, and a transport parameter, which will be introduced through the theory of irreversible thermodynamics. We shall see that the contribution of the transport parameter on cross-diffusion is comparable to that of the thermodynamic parameter. Furthermore, we propose a model based on hydrodynamic volumes, which can be used as a reference for the interpretation of the experimental behavior of cross-diffusion coefficients. It also provides the basis for understanding the magnitude and sign of the thermodynamic and transport parameters. Finally, we examine the role of the aggregation number of micelles and the effect of micelle polydispersity on cross-diffusion parameters.

2. Theory

The main purpose of this section is to introduce two normalized cross-diffusion coefficients, $\tilde{D}_{12}$ and $\tilde{D}_{21}$, that can be directly expressed in terms of fundamental thermodynamic and transport parameters. These can be conveniently examined in dilute solutions according to the formalism of excluded-volume interactions.

To construct $\tilde{D}_{ij}$, we start by making some considerations about concentration scales and reference frames. Eqs. (1a) and (1b) in the previous section were introduced in terms of molar concentrations and corresponding molar fluxes. However, Fick's first law can be also written in terms of mass concentrations and related fluxes. We note that switching concentration scale has no effect on the values of the main-diffusion coefficients because $D_{ii} = -J_i\big|_{\nabla C_j=0}/\nabla C_i$ and the J_i/C_i ratio is independent of concentration scale. On the other hand, the concentration scale needs to be specified for $D_{ij} = -J_i\big|_{\nabla C_i=0}/\nabla C_j$. The value of D_{ij} will also vary depending on the molecular weight chosen to calculate molar concentrations because J_i/C_j is directly proportional to the molecular weight of j and inversely proportional to that of i. However, by introducing the partial molar volumes $\bar{V}_i$ (with $i = 1, 2$), we can appreciate that $(\bar{V}_i/\bar{V}_j)D_{ij}$ is independent of chosen molecular weights since $\bar{V}_i$ is directly proportional to the molecular weight of i. Furthermore, if the mass-concentration scale is employed, then the same value as $(\bar{V}_i/\bar{V}_j)D_{ij}$ is obtained provided that molar volumes are replaced by the corresponding specific volumes. We will include $\bar{V}_i/\bar{V}_j$ as a factor of the definition of $\tilde{D}_{ij}$ proposed below. In this way, the $\tilde{D}_{ij}$ values will be invariant with respect to the aggregation number used to calculate the molar concentration of tyloxapol micelles. Furthermore, molar volumes are convenient parameters for the examination of excluded-volume interactions.

We also note that diffusion can be described relative to different reference frames. For example, in the volume-fixed frame, the fluxes of the components of a ternary system satisfy: $J_0\bar{V}_0 + J_1\bar{V}_1 + J_2\bar{V}_2 = 0$, where the subscript "0" denotes the solvent component. In the solvent-fixed frame, we have: $J_0 = 0$ [46–51]. Since the values of the four diffusion coefficients depend on the chosen reference frame, we need to choose the most convenient reference frame for excluded-volume interactions.

Measured diffusion coefficients correspond, to an excellent approximation, to the volume-fixed frame since volume changes

on mixing are negligible during diffusion experiments [46–48]. This is equivalent to assume that $\bar{V}_i$ is a constant and that mixing occurs within an incompressible fluid at constant volume, pressure and temperature. However, the examination of diffusion coefficients by irreversible thermodynamics often requires converting the obtained volume-fixed diffusion coefficients into the corresponding solvent-fixed diffusion coefficients due to their direct relation to the thermodynamic driving forces, $\nabla\mu_i$, where μ_i (with $i = 1, 2$) are the solute chemical potentials [49,50]. On the other hand, volume-fixed diffusion coefficients require to introduce the linear combinations: $\nabla\mu_i - \gamma_i \nabla\mu_0$ with $\gamma_i \equiv \bar{V}_i/\bar{V}_0$, as the thermodynamic driving forces [47,51].

We now observe that the thermodynamics of excluded-volume interactions in liquid systems is usually described by formally treating the multicomponent liquid mixture, which is assumed to be an incompressible fluid, as an equivalent "gas" mixture [51,52]. Here, the solute chemical potential μ_i is replaced by an effective chemical potential $\tilde{\mu}_i \equiv \mu_i - \gamma_i \mu_0$ of a corresponding gas component and the solvent component is formally removed from the system. This implies that the thermodynamic driving forces of volume-fixed diffusion are the gradients of these effective chemical potentials. We therefore conclude that it is actually convenient to consider diffusion coefficients in the volume-fixed frame when examining excluded-volume interactions.

Normalized cross-diffusion coefficients can be constructed starting from the laws of irreversible thermodynamics. In the volume-fixed frame, the following linear laws can be written:

$$-J_1 = L_{11}\nabla\tilde{\mu}_1 + L_{12}\nabla\tilde{\mu}_2 \tag{2a}$$

$$-J_2 = L_{21}\nabla\tilde{\mu}_1 + L_{22}\nabla\tilde{\mu}_2 \tag{2b}$$

where L_{ij} are the volume-fixed Onsager transport coefficients and $L_{12} = L_{21}$ is the Onsager reciprocal relation [53,54]. Combination of Eqs. (1a) and (1b) and Eqs. (2a) and (2b) leads to

$$D_{11} = L_{11}\tilde{\mu}_{11} + L_{12}\tilde{\mu}_{21} \tag{3a}$$

$$D_{12} = L_{11}\tilde{\mu}_{12} + L_{12}\tilde{\mu}_{22} \tag{3b}$$

$$D_{21} = L_{21}\tilde{\mu}_{11} + L_{22}\tilde{\mu}_{21} \tag{3c}$$

$$D_{22} = L_{21}\tilde{\mu}_{12} + L_{22}\tilde{\mu}_{22} \tag{3d}$$

where $\tilde{\mu}_{ij} \equiv (\partial\tilde{\mu}_i/\partial c_j)_{T,V,c_k,k\neq j}$, and $\tilde{\mu}_{12} = \tilde{\mu}_{21}$ [51]. We now focus on the case of infinite dilution. In the limit of $C_i = 0$, we can write:

$$\tilde{\mu}_{ii} = \frac{\nu_i RT}{C_i} \tag{4a}$$

$$RT\,L_{ii} = \frac{C_i D_i^*}{\nu_i} \tag{4b}$$

$$D_{ii} = L_{ii}\tilde{\mu}_{ii} = D_i^* \tag{4c}$$

where R is the ideal-gas constant, T the absolute temperature and D_i^* the tracer-diffusion coefficient of i, which characterizes particle Brownian mobility [51]. In Eqs. (4a) and (4b), we have introduced the parameter ν_i to take into account the offset between the chosen molar concentration scale for solute i and the corresponding osmolarity. For example, we have $\nu_i > 1$ in the case of a dissociating solute (e.g., strong electrolytes), and $\nu_i < 1$ in the case of an associating solute (e.g., micellar aggregates). Note that ν_1 becomes the reciprocal of the micelle aggregation number when the molecular weight of the surfactant molecule is used to calculate the molar concentration of tyloxapol. If the chosen molar concentration scale matches the corresponding osmolarity, then $\nu_i = 1$ and this parameter may be omitted.

We can combine Eqs. (3a)–(3d) with Eqs. (4a)–(4c) to derive expressions for the dimensionless quotients D_{12}/D_{11} and D_{21}/D_{22}:

$$\frac{D_{ij}}{D_{ii}} = \left(\frac{\tilde{\mu}_{12}}{\nu_i RT} + \frac{\nu_j RT\,L_{12}}{C_1 C_2 D_i^*}\right) C_i \tag{5}$$

Eq. (5) shows that the quotients D_{12}/D_{11} and D_{21}/D_{22} can be expressed as a function of two fundamental parameters: the thermodynamic parameter $\tilde{\mu}_{12}$, and the transport parameter L_{12}. For dilute solutions, the parameters $\tilde{\mu}_{12}$ and $L_{12}/(C_1C_2)$ are independent of concentrations [51]. Thus, D_{12}/D_{11} and D_{21}/D_{22} are directly proportional to C_1 and C_2 respectively. Note that cross-diffusion may result from thermodynamic interactions alone, and $L_{12}/(C_1C_2) = 0$ leads to $D_{ij}/D_{ii} = C_i\,\tilde{\mu}_{12}/(\nu_i RT)$. Our results will show that this approximation cannot be applied.

Based on our previous observations on concentration scales, it is convenient to introduce the normalized (concentration-scale independent, volume-fixed and dimensionless) cross-diffusion coefficient, $\tilde{D}_{ij} \equiv (D_{ij}/D_{ii})(\bar{V}_i/\bar{V}_j)$. Eq. (5) can be then rewritten in the following way:

$$\tilde{D}_{ij} = \left[\Gamma - \left(1 + \frac{D_j^*}{D_i^*}\right)\Lambda\right]\left(\frac{\nu_j}{\gamma_j}\right)\phi_i \tag{6}$$

where $\phi_i = C_i\bar{V}_i$ is the volume fraction of i, $\Gamma \equiv (\tilde{\mu}_{12}/RT)/(\nu_1\nu_2\bar{V}_0)$ is a thermodynamic parameter and $\Lambda \equiv -(RT\,L_{12})/[C_1C_2\bar{V}_0(D_1^* + D_2^*)]$ is a transport parameter. Note that ν_i/γ_i, ϕ_i, Γ and Λ are all parameters independent of the chosen concentration scale.

Our experimental results will be used to determine the slopes: $\tilde{D}_{12}/\phi_1$ and $\tilde{D}_{21}/\phi_2$. These two quantities can be in turn used to determine Γ and Λ. According to Eq. (6), the explicit expressions to extract these two fundamental parameters from experimental $\tilde{D}_{12}/\phi_1$ and $\tilde{D}_{21}/\phi_2$ are

$$\Gamma = \frac{D_1^* D_2^*}{D_2^{*2} - D_1^{*2}}\left[\left(\frac{\gamma_1}{\nu_1}\right)\left(\frac{\tilde{D}_{21}}{\phi_2}\right)\left(1 + \frac{D_2^*}{D_1^*}\right) - \left(\frac{\gamma_2}{\nu_2}\right)\left(\frac{\tilde{D}_{12}}{\phi_1}\right)\left(1 + \frac{D_1^*}{D_2^*}\right)\right] \tag{7a}$$

$$\Lambda = \frac{D_1^* D_2^*}{D_2^{*2} - D_1^{*2}}\left[\left(\frac{\gamma_1}{\nu_1}\right)\left(\frac{\tilde{D}_{21}}{\phi_2}\right) - \left(\frac{\gamma_2}{\nu_2}\right)\left(\frac{\tilde{D}_{12}}{\phi_1}\right)\right] \tag{7b}$$

After extracting Γ and Λ, we can examine their relative importance in the cross-diffusion process. Their values will be then compared to those obtained from a model based on particle hydrodynamic volumes.

3. Materials and methods

3.1. Materials

Tyloxapol (SigmaUltra grade; molecular weight: 4.5 kg mol^{-1}) and poly(ethylene glycol) (PEG; molecular weight: 2.0 kg mol^{-1}) were purchased from Sigma–Aldrich and used without further purification. Deionized water was passed through a four-stage Millipore filter system to provide high purity water (electrical resistivity of 15 MΩ cm) for all the experiments. Stock solutions of tyloxapol-water and PEG-water were made by weight with an error of about 0.1% in their concentrations. Precise masses (±0.0001 g) of stock solutions were added to flasks and diluted with pure water to reach the final target concentrations of the solutions used for the interferometric and light-scattering experiments. Molar concentrations of the solutions were obtained from density. All density measurements were made with a Mettler-Paar

DMA40 density meter, thermostated with water from a large, well-regulated (±1 mK) water bath.

3.2. Rayleigh interferometry

All diffusion measurements were made with the high-precision Gosting diffusiometer operated in its Rayleigh interferometric optical mode. The light source used for generating the Rayleigh interference pattern is a He–Ne Uniphase laser with wavelength $\lambda = 543.5$ nm. A comprehensive description of the Gosting diffusiometer can be found in Ref. [45] and references therein. In brief, a typical diffusion experiment using the Gosting diffusiometer starts from preparing a sharp boundary between two uniform solutions of slightly different solute concentrations located inside a vertical channel with inside width a. In our case, we have: $a = 2.5057$ cm. Rayleigh fringes shift horizontally as the refractive index inside the diffusion channel changes with vertical height. This gives direct information about refractive index, n versus vertical position, x. The difference in refractive index, Δn, between the two solutions is obtained from the total number of fringes J using $\Delta n = J\lambda/a$. We obtain refractive-index profiles at 50 different values of time, t, during the course of each experiment. The experimental refractive-index profile is then described by the normalized anti-symmetric function $f(y) \equiv 2[n(y) - \bar{n}]/\Delta n$, where $y \equiv x/2\sqrt{t}$ and $0 \le f \le 1$. Note that $x = 0$ and time $t = 0$ corresponds to the initial sharp boundary between the two solutions. The values of f within the range: $0.30 \le f \le 0.86$, taking into account the recommendation of Miller and Albright [44].

A comprehensive description on the extraction of binary and ternary diffusion coefficients can be found in Ref. [44] and references therein. Binary diffusion is described by the function: $f = erf(s\,y)$, where $s = D^{-0.5}$ and D is the binary diffusion coefficient. Ternary diffusion is described by the function: $f = \Gamma_1\, erf(s_1\, y) + \Gamma_2\, erf(s_2\, y)$, where s_1 and s_2 are directly related to the two eigenvalues of the diffusion-coefficient matrix, and Γ_1 and $\Gamma_2 = 1 - \Gamma_1$ are the normalized weights of the two observed diffusion modes. Note that a minimum of two experiments is required for determining the four diffusion coefficients at a given set of mean concentrations. These two experiments must have different combinations of solute concentration differences across the diffusion boundary. To verify reproducibility, two other duplicate experiments were performed at each set of mean concentrations. In this paper, multicomponent diffusion coefficients were calculated with respect to solute mass concentrations, c_1 and c_2.

Contrary to the case of the PEG-water binary system, the function $f = erf(s\,y)$ does not satisfactorily describe the observed refractive index profile related to the binary tyloxapol–water system due to tyloxapol polydispersity. Deviation from the ideal binary function is described by the function: $\Omega = erf(s_1\, y) - f$, where $s_1 = \lim_{y\to 0}[erfinv(f)/y]$ and $D_1 = s_1^{-2}$ is a mean diffusion coefficient. In order to take into account tyloxapol polydispersity in diffusion of ternary systems, refractive-index profiles were corrected by applying the procedure described in Ref. [55].

3.3. Light scattering

Measurements of static light scattering were performed at 25.0 ± 0.1 °C. All tyloxapol aqueous samples were filtered through a 0.02 μm filter (Anotop 10, Whatman) and placed in a test tube. The experiments were performed on a light scattering apparatus built using the following main components: He–Ne laser (35 mW, 632.8 nm, Coherent Radiation), manual goniometer and thermostat (Photocor Instruments), multi-tau correlator, APD detector and software (PD4042, Precision Detectors) [39]. All measurements were performed at a scattering angle of 90°. The mass-average molecular weight, M_w, was obtained from the equation: $k_{LS}\, c_1/R_{90} = 1/M_w + 2\,B\,c_1$ [56], where c_1 is the tyloxapol mass concentration, B the second virial coefficient, $k_{LS} = 4\pi^2 n_0^2 (dn/dc_1)^2/(N_A \lambda^4)$, $n_0 = 1.33$ is the refractive index of water, $dn/dc_1 = 0.159$ mL g^{-1} is the refractive index increment for tyloxapol (obtained from the Rayleigh interferometric patterns), N_A is the Avogadro's number, λ is the laser wavelength in vacuum, R_{90} is the excess Rayleigh ratio at 90°. The values of R_{90} were obtained from $R_{90} = (I_s - I_{s,0})/I_{s,R}(n_0^2/n_R^2)\,R_{90,R}$, where I_s is the scattered intensity of the solution, $I_{s,0}$ is the scattered intensity of water, $I_{s,R}$ is the scattering intensity of toluene (the standard) and, $n_R = 1.49$ and $R_{90,R} = 1.35 \times 10^{-5}$ cm^{-1} are the refractive index and the Rayleigh ratio of toluene respectively [57].

4. Results and discussion

The main goal of this paper is to describe cross-diffusion coefficients according to Eq. (6). Since this equation is valid in the limit of infinite dilution, diffusion coefficients were measured at total solute mass concentrations lower than 50 g dm^{-3}. These concentrations were all lower than the crossover concentration (≈100 g dm^{-3}) between dilute and semidilute regimes [58]. Nonetheless, the chosen ternary solute concentrations were sufficiently high for the determination of cross-diffusion coefficients with an error of the order of 10% or lower.

Multicomponent diffusion coefficients $D_{ij}(c_1,c_2)$ for the ternary tyloxapol(1)–PEG(2)–water(0) system at 25 °C are reported in Table 1, as a function of solute mass concentrations, c_i. As described in Section 3, cross-diffusion coefficients are calculated with respect to mass concentrations. Diffusion coefficients for the corresponding binary tyloxapol(1)–water(0) and PEG(2)–water(0) systems are also included. Binary diffusion coefficients will be denoted as D_i in the text. The behavior of our diffusion coefficients will be examined with respect to solute volume fractions, ϕ_i. These were calculated by applying $\phi_i = c_i \bar{v}_1$, where $\bar{v}_1 = 0.885$ cm^{3}g^{-1} and $\bar{v}_2 = 0.840$ cm^{3}g^{-1} are partial specific volumes of tyloxapol [59] and PEG [60] respectively, assumed to be constant within the experimental concentration domain.

4.1. Main-diffusion coefficients

In Fig. 1A, we show the behavior of the diffusion coefficients, D_i, as a function of solute volume fraction, ϕ_i, for the two binary systems. For both systems, the binary diffusion coefficient linearly increases with solute concentration (see Table 1). The increase of the diffusion coefficient with concentration can be attributed to the repulsive nature of particle–particle thermodynamic interactions [60]. This is consistent with a preferential hydration of tyloxapol and PEG molecules. Our binary diffusion measurements were also used to evaluate polydispersity of solute particles in solution. As we will discuss later, tyloxapol micelles are more accurately described as a polydisperse system. On the other hand, polydispersity of PEG chains was found to be relatively small.

The values of tracer-diffusion coefficients of tyloxapol and PEG in water are needed to extract the thermodynamic and transport parameters, Γ and Λ from Eqs. (7a) and (7b). These can be determined from $D_i(\phi_i)$ by linear extrapolation to $\phi_i = 0$ according to $D_i = D_i^*(1 + k_i\phi_i)$. Our results, which are reported in Table 2, are in good agreement with previous studies [59,60]. The tracer-diffusion coefficients, D_i^*, were also used to calculate the hydrodynamic radii of tyloxapol micelles, $R_1^h = 3.57$ nm, and PEG coils, $R_2^h = 1.29$ nm, by applying the Stokes-Einstein equation [61,62], $D_i^* = k_B T/(6\pi\eta R_i^h)$,, where k_B is the Boltzmann constant and $\eta = 0.8902 \times 10^{-3}$ kg m^{-1}s^{-1} is the water viscosity at 25 °C [63].

Table 1
Binary and ternary diffusion coefficients for the Tyloxapol(1)–PEG(2)–water system.

c_1/g dm^{-3}	c_2/g dm^{-3}	$D_{11}/10^{-9}$ m^2 s^{-1}	$D_{12}/10^{-9}$ m^2 s^{-1}	$D_{21}/10^{-9}$ m^2 s^{-1}	$D_{22}/10^{-9}$ m^2 s^{-1}
4.545	0	0.0692 ± 0.0002[a]	–	0	–
9.999	0	0.0701 ± 0.0002[a]	–	0	–
20.00	0	0.0711 ± 0.0002[a]	–	0	–
0	5.000	–	0	–	0.1919 ± 0.0005[a]
0	10.01	–	0	–	0.1911 ± 0.0005[a]
0	19.96	–	0	–	0.1944 ± 0.0005[a]
4.545	4.536	0.0677 ± 0.0002	0.0072 ± 0.0005	0.0031 ± 0.0009	0.1901 ± 0.0005
10.01	9.054	0.0657 ± 0.0003	0.0164 ± 0.0005	0.0076 ± 0.0009	0.1877 ± 0.0005
20.00	20.00	0.0615 ± 0.0003	0.0306 ± 0.0005	0.0133 ± 0.0009	0.1874 ± 0.0005
9.999	5.000	0.0668 ± 0.0003	0.0164 ± 0.0005	0.0044 ± 0.0009	0.1870 ± 0.0005
4.541	9.052	0.0656 ± 0.0004	0.0063 ± 0.0005	0.0058 ± 0.0009	0.1923 ± 0.0005
20.00	5.000	0.0684 ± 0.0002	0.0322 ± 0.0005	0.0040 ± 0.0009	0.1815 ± 0.0005
4.545	16.26	0.0614 ± 0.0003	0.0068 ± 0.0005	0.0124 ± 0.0009	0.1946 ± 0.0005

[a] Binary values D_1 and D_2 are denoted as D_{11} and D_{22} respectively.

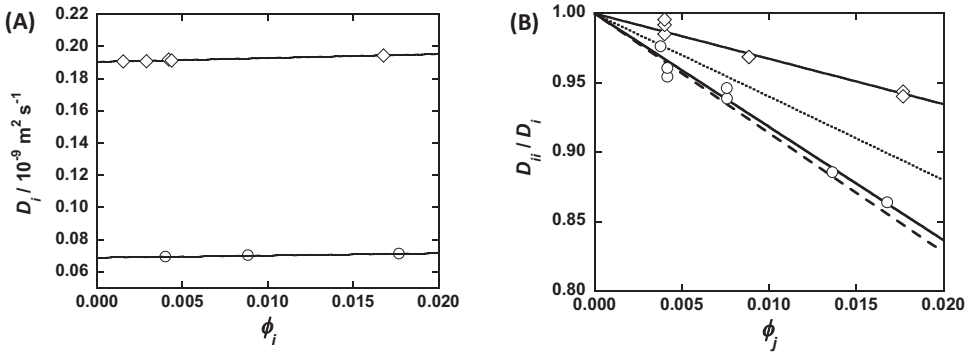

Fig. 1. (A) Binary diffusion coefficient, D_1 (circles) and D_2 (diamonds) as a function of solute volume fraction, ϕ_1 and ϕ_2, for the tyloxapol(1)–water and PEG(2)–water systems. The solid lines are linear fits through the data. (B) Normalized ternary main-diffusion coefficient, $D11/D1$ (circles) and D_{22}/D_2 (diamonds), as a function of solute volume fraction, ϕ_2 and ϕ_1, for the tyloxapol(1)–PEG(2)–water ternary system. The solid lines are linear fits through the data. The dashed lines represent $D_{11}/D_1 = (1 + 8.53\phi_2 + 101\phi_2{}^2)^{-1}$ (- - -) and $D_{22}/D_2 = (1 + 11.4\,\phi_1)^{-1}$ (····), where $(1 + 8.53\phi_2 + 101\phi_2{}^2)$ and $(1 + 11.4\phi_1)$ were obtained by applying the method of least squares to relative-viscosity data of PEG–water and tyloxapol–water systems respectively.

The extracted value of R_1^h is in good agreement with the diameter of 7 nm of spherical tyloxapol micelles observed by microscopy [42].

The behavior of the two ternary diffusion coefficient can be examined by plotting ternary-to-binary ratios, D_{ii}/D_i, as a function of ϕ_j,, the volume fraction of the other solute. As we can see in Fig. 1B, D_{ii}/D_i decreases as ϕ_j increases, the effect being larger for tyloxapol diffusion in the presence of PEG. Furthermore, D_{ii}/D_i can be regarded as independent of ϕ_i within the experimental error. The decrease of D_{ii}/D_i is stronger for the case of tyloxapol diffusion in the presence of PEG. We have applied the method of linear least squares to fit our data with $D_{ii}/D_i = 1 - k_{ij}\,\phi_j$. Our values of k_{ij} are reported in Table 2.

Since D_{ii}/D_i can be regarded as independent of ϕ_i, we can write: $D_{ii} = D_i^*(1 - k_{ij}\,\phi_j)(1 + k_i\,\phi_i)$ and the slope k_{ij} describes the effect of a crowding solute on the mobility of a single Brownian particle (i.e. when $\phi_i = 0$). This is given by $D_i^*(1 - k_{ij}\,\phi_j)$. According to the Stokes-Einstein equation, the friction experienced by a Brownian particle is directly proportional to the viscosity of the surrounding fluid. In our case, this consists of water and the crowding solute with volume fraction, ϕ_j. Thus, the observed decrease in particle mobility may be attributed to a corresponding increase in viscosity. In Fig. 1B, we show the behavior of D_{ii}/D_i predicted from relative-viscosity data [64,65] as dashed lines. In both cases, we can see that viscosity predicts a larger than observed decrease in D_{ii}/D_i.

Table 2
Parameters in the main-diffusion coefficients, $D_{ii} = D_i^*(1 - k_{ij}\phi_j)(1 + k_i\phi_i)$, and slopes, $\tilde{D}_{ij}/\phi_i$, of the normalized cross-diffusion coefficients extracted by applying the method of least squared to experimental results.

$D_1^*/10^{-9}$ m^2 s^{-1}	0.0688 ± 0.0002
$D_2^*/10^{-9}$ m^2 s^{-1}	0.1904 ± 0.0002
k_1	1.98 ± 0.27
k_2	1.28 ± 0.15
k_{12}	8.17 ± 0.27
k_{21}	3.27 ± 0.16
$\tilde{D}_{12}/\phi_1$	29.0 ± 0.3
$\tilde{D}_{21}/\phi_2$	4.2 ± 0.2

Stokes-Einstein equation assumes that the fluid surrounding the Brownian particle can be treated as a continuum. However, this is expected to be a good approximation only for diffusion of large molecules in the presence of small solvent molecules. If a crowding agent has a size comparable or larger than the Brownian particle under investigation, the heterogeneity of the surrounding fluid may become important. Since tyloxapol micelles are significantly larger than PEG coils, the assumption of continuum fluid is expected to describe the mobility of a tyloxapol micelle in the presence of PEG better than the mobility of a PEG coil in the presence of tyloxapol. This is in agreement with our plots in Fig. 1B. Furthermore, we can see that the friction experienced by a particle, when it diffuses through a crowded fluid, is lower compared to the continuum prediction. This can be explained by invoking depletion effects [66,67]. In other words, depletion of a crowding solute from the surface of a particle leads to a low-viscosity layer around the particle as compared to the viscosity in the bulk solution.

4.2. Cross-Diffusion coefficients

We now turn our attention to cross-diffusion. In Fig. 2, we show the behavior of the normalized cross-diffusion coefficients, $\tilde{D}_{ij}$ as a function of ϕ_i. In both cases, $\tilde{D}_{ij}$ linearly increases with ϕ_i starting

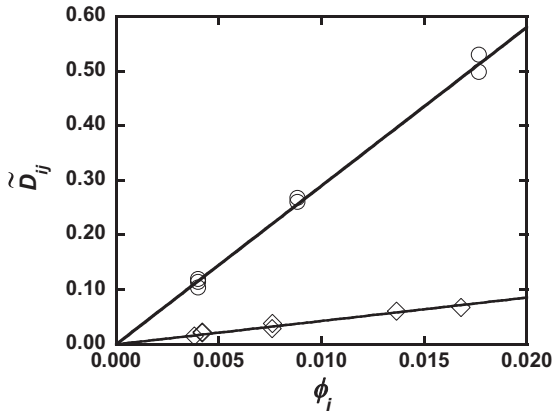

Fig. 2. Normalized ternary cross-diffusion coefficient, $\tilde{D}_{12}$ (circles) and $\tilde{D}_{21}$ (diamonds), as a function of solute volume fraction, ϕ_1 and ϕ_2, for the tyloxapol(1)–PEG(2)–water system. The solid lines are linear fits through the data.

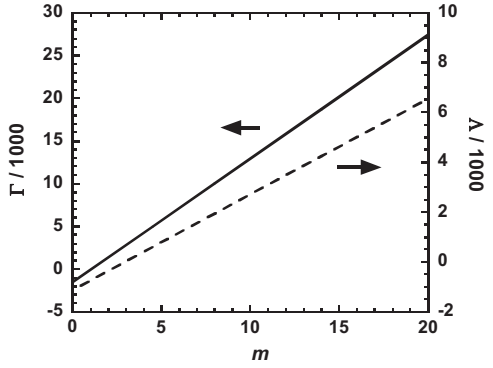

Fig. 3. Thermodynamic parameter, Γ (solid line), and transport parameter, Λ (dashed line), calculated as a function of the aggregation number of tyloxapol micelles, *m*.

from $\tilde{D}_{ij} = 0$ at $\phi_i = 0$. Note that $\tilde{D}_{ij}$ can be regarded as independent of the volume fraction of the other solute, ϕ_j, within the experimental error. The two values of $\tilde{D}_{ij}/\phi_i$ reported in Table 2 were obtained by applying the method of linear least squares to our experimental data. Our results indicate that the thermodynamic and transport parameters Γ and Λ in Eq. (6) can be assumed constant.

The application of Eqs. (7a) and (7b) requires the knowledge of γ_i/ν_i. Specific volumes and molecular weights of tyloxapol, PEG and water allow us to calculate the corresponding molar volumes: $\bar{V}_1 = 3.98$ dm^{3}mol^{-1}, $\bar{V}_2 = 1.68$ dm^{3}mol^{-1} and $\bar{V}_0 = 0.01807$ dm^{3}mol^{-1}. If we neglect small polydispersity effects, PEG molar weight corresponds to the mass of the actual coil. Thus, we set: $\nu_2 = 1$ and calculate: $\gamma_2/\nu_2 = 93.0$. On the other hand, the molar weight of tyloxapol corresponds to one tyloxapol unit and not to the actual mass of its micelles. Thus, we set: $\nu_1 = 1/m$, where m is the micelle aggregation number. For tyloxapol, we consider how the calculated γ_1/ν_1 changes depending on the chosen value of m and write: $\gamma_1/\nu_1 = 220\,m$. Note that the slope of $\tilde{D}_{12}$ in Fig. 2 is significantly larger than that of $\tilde{D}_{21}$. This can be mostly attributed to γ_1/ν_1 being larger than γ_2/ν_2 in Eq. (6).

In Fig. 3, we show the thermodynamic and transport parameters Γ and Λ calculated from Eqs. (7a) and (7b) as a function of the micelle aggregation number, *m*. This figure allows us to appreciate how the values of these two parameters depend on the choice of *m*. If we incorrectly consider the case of $m = 1$ ignoring the formation of micelles, we obtain negative values Γ and Λ. On the contrary, we must consider relatively larger values of *m* and conclude that Γ and Λ should be both positive. Another important result we can deduce from Fig. 3 is the relative contribution of Λ compared to Γ in $\tilde{D}_{ij}$ (see Eq. (6)). As we shall see later in this paper, the mean number-average and mass-average aggregation numbers of tyloxapol micelles are 7.0 and 11.4 respectively. If we consider these values of *m* in Fig. 3, we calculate $\Gamma = 8600$ and $\Lambda = 1600$ for $m = 7.0$, and $\Gamma = 15,000$ and $\Lambda = 3300$ for $m = 11.4$. Both cases allow us to conclude that the term containing Λ in Eq. (6) is 69–83% and 25–30% of Γ in the case of $\tilde{D}_{12}$ and $\tilde{D}_{21}$ respectively. Thus, cross-diffusion cannot be approximately described solely as a thermodynamic phenomenon, and the Onsager transport coefficient, L_{12}, cannot be neglected, especially in the case of D_{12}, which describes the cross-diffusion flux of the faster-diffusing solute.

4.3. Hydrodynamic-volume model for Γ and Λ

We now introduce theoretical expressions of the thermodynamic and transport parameters Γ and Λ for a reference hard-sphere model. The advantage of this model is that the calculation of Γ and Λ is based on the values of the tracer-diffusion coefficients, D_i^*, and the solvent molar volume only. Clearly deviations for systems containing polymer coils or more complex macromolecules are expected. Nonetheless, a reference model based on hard spheres is preferred due to its relative simplicity. Specifically, the relation between D_i^* and the corresponding hydrodynamic volume is straightforward, and the effects of excluded-volume interactions on Γ can be easily described for a hard-sphere system. The proposed model allows us to obtain reference values for our experimental results on Γ and Λ. In the following analysis, we shall set $\nu_1 = \nu_2 = 1$ since our model will directly consider the molar concentrations, C_i, of the actual diffusing species in solution.

In the case of Γ, we start by considering a well-established excluded-volume model based on impenetrable hard spheres. Due to excluded-volume interactions, the effective chemical potential of a solute is given by $(\tilde{\mu}_i - \tilde{\mu}_i^0)/RT = \ln(C_i/\alpha_j)$, where $\tilde{\mu}_i^0$ is the chemical potential in the standard state and α_j is the free-volume fraction [6]. The thermodynamic activity, C_i/α_j, is the molar concentration of the solute particles in the free volume. For a particle *i* in the presence of a crowding solute *j*, we can write: $\alpha_j = 1 - V_{ex}C_j$ in the limit of low C_j, where V_{ex} is the excluded volume. Differentiation of $\tilde{\mu}_i$ allows us to obtain: $\tilde{\mu}_{12}/RT = V_{ex}$ [51]. If we treat both solutes as hard spheres, and assume that their volumes coincide with the corresponding hydrodynamic volumes, V_i^h, we obtain: $V_{ex} = [(V_1^h)^{1/3} + (V_2^h)^{1/3}]^3$. The corresponding expression of Γ is then given by

$$\Gamma = \frac{[(V_1^h)^{1/3} + (V_2^h)^{1/3}]^3}{\bar{V}_0} \tag{8}$$

Note that Γ in Eq. (8) is described as the excluded volume normalized with respect to the volume of solvent molecules. The hydrodynamic radii extracted from the Stokes-Einstein equation can be used to calculate the hydrodynamic volumes of tyloxapol and PEG, $V_1^h = 114$ dm^{3}mol^{-1} and $V_2^h = 5.40$ dm^{3}mol^{-1} respectively. Thus, we obtain $\Gamma = 15,900$ from Eq. (8), a value that is comparable with our results in Fig. 3 for aggregation numbers of the order of 10.

In the case of Λ, we will consider the theory developed in Ref. [51]. It can be shown that the expression: $RT\,L_{12} = -C_1C_2(V_1^hD_1^* + V_2^hD_2^*)$ follows from solute hydration. This relation assumes that the contribution of other sources of solute-solute interactions to L_{12} can be neglected, which may become accurate when solute

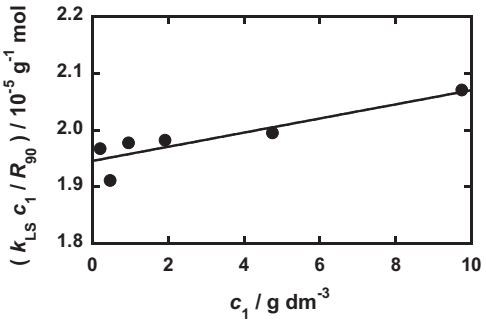

Fig. 4. Static-light-scattering data for the binary tyloxapol-water system as a function of solute mass concentration, c_1. Experimental data were fitted by applying the Debye linear equation: $k_{LS}c_1/R_{90} = 1/M_w + 2Bc_1$, where R_{90} is the excess Rayleigh ratio at 90°, k_{LS} is an optical constant (see Section 3 for more details), $M_w = 51.4 \pm 0.4$ kg mol^{-1} is mass-average molecular weight of the tyloxapol micelles and $B = (6.2 \pm 1.6) \times 10^{-8}$ mol L g^{-2} is the corresponding second virial coefficient.

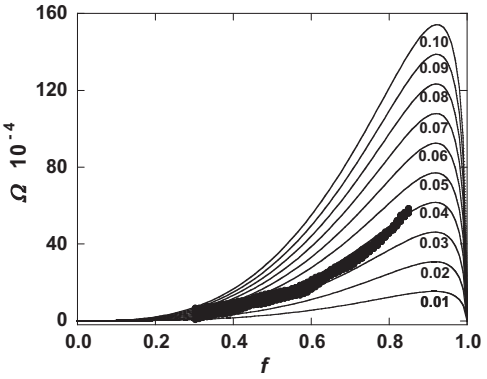

Fig. 5. Experimental deviation function, Ω, as a function of the normalized refractive-index profile, f, for the binary tyloxapol-water system. The solid curves are computed as a function of the polydispersity index, ω (numbers associated with each curve), by applying the three-species model described in the text.

hydration is large. The corresponding expression of Λ is then given by

$$\Lambda = \frac{D_1^* V_1^h + D_2^* V_2^h}{(D_1^* + D_2^*)\bar{V}_0} \quad (9)$$

Note that Λ in Eq. (9) is described as a weighted-average hydrodynamic volume normalized with respect to the volume of solvent molecules. We obtain $\Lambda = 1900$ from Eq. (9) by using our tracer-diffusion coefficients and corresponding hydrodynamic volumes. As we can see in Fig. 3, also Λ is comparable with our experimental results for aggregation numbers of the order of 10. Thus, we believe that the proposed expressions for Γ and Λ capture the most important factors responsible for the observed behavior of cross-diffusion.

In summary, the comparison between our experimental results in Fig. 3 and the proposed reference model based on hydrodynamic volume of hard spheres indicates that excluded-volume interactions and solute hydration represent the main contributions to the experimental behavior of $\tilde{D}_{12}$ and $\tilde{D}_{21}$. However, a precise quantitative comparison requires knowledge of both aggregation number and polydispersity of tyloxapol micelles. Since these are often traits of macromolecular and colloidal systems, it becomes interesting to examine their impact on the relation of cross-diffusion coefficients to fundamental thermodynamic and transport parameters. This will be addressed in the following section.

4.4. Aggregation number and polydispersity of tyloxapol micelles

Regev and Zana determined the values of the tyloxapol aggregation number, $m = 9.1$ and $m = 14$ at 40 °C and 55 °C respectively, using time-resolved fluorescence quenching [42]. However, the corresponding value at 25 °C is not currently available. To determine m at 25 °C, we have performed measurements of static light scattering and determined the micelle molecular weight through the Debye plot shown in Fig. 4. We have obtained the molecular weight of 51.4 kg mol^{-1} corresponding to $m = 11.4$.

It is interesting to observe that the light-scattering value is higher than that reported by Regev and Zana. This might be surprising since tyloxapol aggregation is expected to be enhanced as temperature increases [42]. We have attributed this apparent discrepancy to polydispersity of tyloxapol micelles. In other words, the light-scattering value of m corresponds to the mass-average molar weight [56] and will overestimate that obtained by several other techniques.

Hydrodynamic measurements should provide an accurate description of micelle polydispersity. Indeed, other more precise techniques such as mass spectrometry can be only applied to characterize molecular-weight polydispersity of surfactant molecules. However, it is a very challenging task to convert the surfactant molecular-weight polydispersity into the corresponding micelle polydispersity in water. Thus, we have used our binary diffusion measurements to characterize hydrodynamic-radius polydispersity. Our general approach to characterize polydispersity, which has been described in Ref. [55], is based on the examination of the normalized refractive-index profile, $f(y)$, of the binary tyloxapol-water system (see Section 3 for the definition of $f(y)$). Polydispersity can be characterized by considering the deviation function $\Omega(f)$ from an ideal monodisperse system. As previously described, a simple analysis of diffusion polydispersity can be performed by considering a three-species model system [55]. The three diffusing species in this model have diffusion coefficients: $D_1^{*(1)} = D_1^*/(1+\omega^{0.5})^2$, $D_1^{*(2)} = D_1^*$ and $D_1^{*(3)} = D_1^*/(1-\omega^{0.5})^2$, where ω is a parameter that quantifies the extent of polydispersity. The corresponding weight fractions are chosen to be $w_1^{(1)} = 1/6$, $w_1^{(2)} = 2/3$, and $w_1^{(3)} = 1/6$ so that D_1^* is the mean diffusion coefficient given by $D_1^* \equiv [\sum_i w_1^{(i)}/(D_1^{*(i)})^{0.5}]^{-2}$, and the diffusion-based polydispersity index follows the definition: $\omega \equiv [\sum_i w_1^{(i)}/(D_1^{*(i)})^{1.5}]/[\sum_i w_1^{(i)}/(D_1^{*(i)})^{0.5}]^3 - 1$ [55]. In Fig. 5, we plot the experimental $\Omega(f)$ for tyloxapol together with that calculated from our three-species model as a function of the polydispersity index, ω. As we can see from this figure, the best agreement is obtained for $\omega = 0.04$.

To estimate the number-average aggregation number, we can convert this value of ω into the corresponding M_w/M_n, where M_n and M_w are the number-average and mass-average molecular weights respectively. We first calculate the three diffusion coefficients $D_1^{*(k)}$ of this model system from $\omega = 0.04$ and $D_1^* = 0.0688 \times 10^{-9}$ m^{2}s^{-1}. If we then treat micelles as globular particles and observe that particle radius is inversely proportional to its tracer-diffusion coefficient, we can write: $D_1^{*(k)} \propto M_k^{-1/3}$, where M_k is the molecular weight of micelle k. This assumption allows us to estimate $M_w/M_n = 1.6$. This polydispersity index can be used to extract the number-average aggregation number of 7.0 from our light-scattering results. This value is qualitatively consistent with those reported by Regev and Zana [42].

We now show how to calculate precise values of Γ and Λ from Eqs. (7a) and (7b). We start by examining the role of polydispersity on cross-diffusion coefficients. We shall introduce equations for the two measurable $\tilde{D}_{ij}$ by considering polydispersity of one solute only (solute 1). Polydispersity of this solute is described by a set of weight fractions $w_1^{(k)}$ with $k = 1, 2, 3, \ldots$ Theoretical considerations based on Ref. [55] together with the definition of $\tilde{D}_{ij}$ introduced in this paper allow us to write the following expressions for $\tilde{D}_{ij}$:

$$\tilde{D}_{12} = \sum_k \left(\frac{D_1^{*(k)}}{D_1^*} \right) \tilde{D}_{12}^{(k)} \tag{10a}$$

$$\tilde{D}_{21} = \sum_k w_1^{(k)} \tilde{D}_{21}^{(k)} \tag{10b}$$

where $\phi_1^{(k)}$ is the volume fraction of micelle k with $\phi_1 = \sum_k \phi_1^{(k)}$ and $\phi_1^{(k)} = w_1^{(k)} \phi_1$, $D_1^{*(k)}$ is the tracer-diffusion coefficient of micelle k with $D_1^* \equiv [\sum_i w_1^{(i)} / (D_1^{*(i)})^{0.5}]^{-2}$, $\tilde{D}_{12}^{(k)} \equiv (D_{12}^{(k)}/D_{11}^{(k)})(\bar{V}_1^{(k)}/\bar{V}_2)$ and $\tilde{D}_{21}^{(k)} \equiv (D_{21}^{(k)}/D_{22})(\bar{V}_2/\bar{V}_1^{(k)})$ are the normalized cross-diffusion coefficients between micelle k and PEG. The partial molar volume of the micelle k, $\bar{V}_1^{(k)}$, is calculated by using the reasonable assumption that the micelle specific volume is independent of k. Note that Eq. (10a) describes $\tilde{D}_{12}$ as a sum of cross-diffusion contributions. On the other hand, Eq. (10b) describes $\tilde{D}_{21}$ as a weighted average of individual cross-diffusion contributions.

According to Eq. (6) with $\nu_1 = \nu_2 = 1$, we can write:

$$\tilde{D}_{12}^{(k)} = \left[\Gamma^{(k)} - \left(1 + \frac{D_2^*}{D_1^{*(k)}} \right) \Lambda^{(k)} \right] \left(\frac{1}{\gamma_2} \right) \phi_1^{(k)} \tag{11a}$$

$$\tilde{D}_{21}^{(k)} = \left[\Gamma^{(k)} - \left(1 + \frac{D_1^{*(k)}}{D_2^*} \right) \Lambda^{(k)} \right] \left(\frac{1}{\gamma_1^{(k)}} \right) \phi_2 \tag{11b}$$

where $\gamma_1^{(k)} \equiv \bar{V}_1^{(k)}/\bar{V}_0$, $\Gamma^{(k)} \equiv (\tilde{\mu}_{12}^{(k)}/RT)/\bar{V}_0$, $\Lambda^{(k)} \equiv -(RT\, L_{12}^{(k)})/[C_1^{(k)} C_2 \bar{V}_0 (D_1^{*(k)} + D_2^*)]$ and $C_1^{(k)}$ is the molar concentration of micelle k. Substitution of Eqs. (11a) and (11b) into Eqs. (10a) and (10b) yields:

$$\tilde{D}_{12} = \left[\Gamma - \left(1 + \frac{D_2^*}{D_1^*} \right) \Lambda \right] \left(\frac{1}{\gamma_2} \right) \phi_1 \tag{12a}$$

$$\tilde{D}_{21} = \left[\Gamma' - \left(1 + \frac{D_1^*}{D_2^*} \right) \Lambda' \right] \left(\frac{1}{\gamma_1} \right) \phi_2 \tag{12b}$$

where we have introduced the following mean thermodynamic and transport coefficients: $\Gamma \equiv (1/D_1^*) \sum_k w_1^{(k)} \Gamma^{(k)} D_1^{*(k)}$ and $\Lambda \equiv \sum_i w_1^{(k)} (D_1^{*(k)} + D_2^*) \Lambda^{(k)} / (D_1^* + D_2^*)$ in the expression of $\tilde{D}_{12}$, and $\Gamma' \equiv \gamma_1 \sum_k w_1^{(k)} \Gamma^{(k)} / \gamma_1^{(k)}$, $\Lambda' \equiv [\gamma_1/(D_1^* + D_2^*)] \sum_i [w_1^{(k)} (D_1^{*(k)} + D_2^*) \Lambda^{(k)} / \gamma_1^{(k)}]$ and $\gamma_1 \equiv 1 / \sum_k w_1^{(k)} / \gamma_1^{(k)}$ in the expression of $\tilde{D}_{21}$. Since $\gamma_1^{(k)} \propto M_k$, γ_1 is the number average of the $\gamma_1^{(k)}$ values.

It is interesting to observe that $\Gamma \neq \Gamma'$ and $\Lambda \neq \Lambda'$ due to polydispersity. This implies that $\tilde{D}_{12}/\phi_1$ and $\tilde{D}_{21}/\phi_2$ may not be used to extract all four coefficients unless the ratios Γ'/Γ and Λ/Λ' are known. These ratios can be estimated by applying our hydrodynamic-volume model based on Eqs. (8) and (9) to the three-species system with $\omega = 0.04$. We shall assume that the hydrodynamic volume of a micelle is directly proportional to its molecular weight. Note that the calculated Γ'/Γ and Λ/Λ' will not depend on the absolute values of hydrodynamic volumes but on their relative ratios only.

To estimate the ratios Γ'/Γ and Λ/Λ', we first utilize the three previously calculated $D_1^{*(k)}$ to determine the corresponding hydrodynamic volumes from the Stokes-Einstein equation. We then insert these values into Eqs. (8) and (9) to obtain $\Gamma^{(k)}$ and $\Lambda^{(k)}$ of the three species. The number-average $\gamma_1 = 1530$ was directly calculated from the micelle number-average aggregation number. We are now in position to calculate $\Gamma'/\Gamma = 0.741$ and $\Lambda/\Lambda' = 0.744$. Since $\Gamma'/\Gamma \cong \Lambda/\Lambda'$, Eqs. (7a) and (7b) can be still used to determine Γ and Λ provided that γ_1 is replaced by $\gamma_1/0.74$. This allows us to extract $\Gamma = 12,000$ and $\Lambda = 2500$, which correspond to $m = 9.5$ in Fig. 3. These values are respectively 28% lower and 23% higher than those calculated from the reference hydrodynamic-volume model.

The lower experimental value of Γ compared to that predicted from the hydrodynamic-volume model can be attributed to the deformability of PEG coils and the soft nature of the outer shell of tyloxapol micelles, which also consist of poly(ethylene glycol) chains. Thus, a partial overlap between these particles can occur thereby yielding an excluded volume smaller than that predicted from their hydrodynamic volumes. On the other hand, we were unable to identify a mechanism responsible for the relatively high experimental value of Λ. Furthermore, the friction-based formalism of Onsager transport coefficients [51,68] and empirical estimations of friction coefficients [69] indicate that the value of Λ should be lower than that calculated from the proposed hydrodynamic-volume model. Although our investigation has shown the importance of Λ in cross-diffusion and its relation to solute hydration, more theoretical and experimental diffusion studies are needed to identify other factors influencing the value of this transport parameter.

5. Summary and conclusions

We have reported the four multicomponent diffusion coefficients for the tyloxapol-PEG-water system. Our investigation has focused on the behavior of the two normalized cross-diffusion coefficients, $\tilde{D}_{ij}$, as a function of ϕ_i. The slopes $\tilde{D}_{ij}/\phi_i$ were used to extract the thermodynamic parameter, Γ, and the transport parameter, Λ. These parameters are both positive consistent with solute(1)–solute(2) thermodynamic excluded-volume interactions and solute hydration. Our results show that cross-diffusion cannot be approximately described as a mere thermodynamic phenomenon since the magnitude of Γ is comparable to that of Λ. We have proposed a reference hydrodynamic-volume model based on hard spheres for our experimental studies. This model indicates that excluded-volume thermodynamic interactions and particle hydration represent the main contributions to the experimental behavior of cross-diffusion. However, a precise determination of Γ and Λ requires the knowledge of the micelle aggregation number and polydispersity. Thus, we have examined the effect of aggregation and polydispersity, and quantitatively determined the discrepancy between experimental results and reference model. This work provides the basis for further experimental and theoretical cross-diffusion studies on this class of systems.

Acknowledgments

The authors thank John G. Albright for technical assistance with the Gosting diffusiometer. This work was supported by the ACS Petroleum Research Fund (47244-G4) and TCU Research and Creative Activity Funds.

References

[1] W.B. Russel, D.A. Saville, W.R. Schowalter, Colloidal Dispersions, Cambridge University Press, New York, 1989.
[2] H.N.W. Lekkerkerker, R. Tuinier, Colloids and the Depletion Interaction (Lecture Notes in Physics Vol. 833), Springer, Dordrecht, 2011.
[3] D.H. Napper, Polymeric Stabilisation of Colloidal Dispersions, Academic Press, London, 1983.
[4] S. Asakura, F. Oosawa, On interaction between two bodies immersed in a solution of macromolecules, J. Chem. Phys. 22 (1954) 1255–1256.
[5] S. Asakura, F. Oosawa, Interaction between particles suspended in solutions of macromolecules, J. Polym. Sci. 33 (1958) 183–192.
[6] H.N.W. Lekkerkerker, W.C.K. Poon, P.N. Pusey, A. Stroobants, P.B. Warren, Phase behaviour of colloid + polymer mixtures, Europhys. Lett. 20 (1992) 559–564.
[7] S.M. Ilett, A. Orrock, W.C.K. Poon, P.N. Pusey, Phase behaviour of a model colloid–polymer mixture, Phys. Rev. E 51 (1995) 1344–1352.
[8] H.-X. Zhou, G. Rivas, A.P. Minton, Macromolecular crowding and confinement: Biochemical, biophysical, and potential physiological consequences, Ann. Rev. Biophys. 37 (2008) 375–397.
[9] R.J. Ellis, Macromolecular crowding: obvious but underappreciated, Trends Biochem. Sci. 26 (2001) 597–604.
[10] J. Schwarz-Linek, C. Valeriani, A. Cacciuto, M.E. Cates, D. Marenduzzo, A.N. Morozov, W.C.K. Poon, Phase separation and rotor self-assembly in active particle suspensions, Proc. Natl. Acad. Sci. U.S.A. 109 (2012) 4052–4057.
[11] J. Zhou, J.S. van Duijneveldt, B. Vincent, Two-stage phase separation in ternary colloid–polymer mixtures, Phys. Chem. Chem. Phys. 13 (2011) 110–113.
[12] O. Annunziata, N. Asherie, A. Lomakin, J. Pande, O. Ogun, G.B. Benedek, Effect of polyethylene glycol on the liquid–liquid phase transition in aqueous protein solutions, Proc. Natl. Acad. Sci. U.S.A. 99 (2002) 14165–14170.
[13] D.G. Kanjickal, S.T. Lopina, Modeling of drug release from polymeric delivery systems, Crit. Rev. Ther. Drug Carr. Syst. 21 (2004) 345–386.
[14] J.A. Wesselingh, Controlling diffusion, J. Control. Rel. 24 (1993) 47–60.
[15] J.T.F. Keurentjes, A.E.M. Janssena, A.P. Broeka, A. Van der Padta, J.A. Wesselingh, K. Van 'T Riet, Multicomponent diffusion in dialysis membranes, Chem. Eng. Sci. 47 (1992) 1963–1971.
[16] B. Abécassis, C. Cottin-Bizonne, C. Ybert, A. Ajdari, L. Bocquet, Boosting migration of large particles by solute contrasts, Nat. Mater. 7 (2008) 785–789.
[17] B.H. Weigl, P. Yager, Microfluidics, Microfluidic diffusion-based separation and detection, Science 283 (1999) 346–347.
[18] D.N. Petsev, K. Chen, O. Gliko, P.G. Vekilov, Diffusion-limited kinetics of the solution-solid phase transition of molecular substances, Proc. Natl. Acad. Sci. U.S.A. 100 (2003) 792–796.
[19] J.M. Garcia-Ruiz, Counterdiffusion methods for macromolecular crystallization, Meth. Enzym. 368 (2003) 130–154.
[20] D.G. Miguez, V.K. Vanag, I.R. Epstein, Fronts and pulses in an enzymatic reaction catalyzed by glucose oxidase, Proc. Natl. Acad. Sci. U.S.A. 104 (2007) 6992–6997.
[21] S. Park, N. Agmon, Concentration profiles near an activated enzyme, J. Phys. Chem. B 112 (2008) 12104–12114.
[22] M. Postma, P.J.M. Van Haastert, A diffusion-translocation model for gradient sensing by chemotactic cells, Biophys. J. 81 (2001) 1314–1323.
[23] R.G. Thorne, A. Lakkaraju, E. Rodriguez-Boulan, C. Nicholson, In vivo diffusion of lactoferrin in brain extracellular space is regulated by interactions with heparan sulfate, Proc. Natl. Acad. Sci. U.S.A. 105 (2008) 8416–8421.
[24] K.A. Sochacki, I.A. Shkel, M.T. Record, J.C. Weisshaar, Protein diffusion in the periplasm of *E-coli* under osmotic stress, Biophys. J. 100 (2011) 22–31.
[25] J.A. Dix, A.S. Verkman, Crowding effects on diffusion in solutions and cells, Ann. Rev. Biophys. 37 (2008) 247–263.
[26] F. Roosen-Runge, M. Hennig Marcus, F. Zhang, R.M.J. Jacobs, M. Sztucki, H. Schober, T. Seydel, F. Schreiber, Protein self-diffusion in crowded solutions, Proc. Natl. Acad. Sci. U.S.A. 108 (2011) 11815–11820.
[27] A. Vergara, F. Capuano, L. Paduano, R. Sartorio, Lysozyme mutual diffusion in solutions crowded by poly(ethylene glycol), Macromolecules 39 (2006) 4500–4506.
[28] H.J.V. Tyrrell, K.R. Harris, Diffusion in Liquids, Butterworths, London, 1984.
[29] A. Vergara, L. Paduano, R. Sartorio, Mechanism of protein-poly(ethylene glycol) interaction from a diffusive point of view, Macromolecules 35 (2002) 1389–1398.
[30] A. Vergara, L. Paduano, R. Sartorio, Multicomponent diffusion in systems containing molecules of different size - Part 3. Mutual diffusion in the ternary system hexa(ethylene glycol)-di(ethylene glycol)-water, Phys. Chem. Chem. Phys. 3 (2001) 4340–4345.
[31] O. Annunziata, A. Vergara, L. Paduano, R. Sartorio, D.G. Miller, J.G. Albright, Quaternary diffusion coefficients in a Protein–Polymer–Salt–Water system determined by Rayleigh interferometry, J. Phys. Chem. B 113 (2009) 13446–13453.
[32] H.M. Halvorsen, E. Wygnal, M.R. MacIver, D.G. Leaist, Ternary mutual diffusion coefficients from error-function dispersion profiles: aqueous solutions of triton X-100 micelles plus poly(ethylene glycol), J. Chem. Eng. Data 52 (2007) 442–448.
[33] H.M. Halvorsen, D.G. Leaist, An electrostatic mechanism for the coupled diffusion of polymer molecules and ionic micelles. Aqueous poly(ethylene glycol) plus sodium dodecyl sulfate solutions, Phys. Chem. Chem. Phys. 6 (2004) 3515–3523.
[34] P.A. Albertsson, Partition of Cell Particles and Macromolecules, Wiley, New York, 1986.
[35] A. McPherson, Crystallization of Biological Macromolecules, Cold Spring Harbor, New York, 1998.
[36] M.J. Roberts, M.D. Bentley, J.M. Harris, Chemistry for peptide and protein PEGylation, Adv. Drug. Deliv. Rev. 54 (2002) 459–476.
[37] R. Bhat, S.N. Timasheff, Steric exclusion is the principal source of the preferential hydration of proteins in the presence of polyethylene glycols, Protein Sci. 1 (1992) 1133–1143.
[38] A. Tardieu, F. Bonnete, S. Finet, D. Vivares, Understanding salt or PEG induced attractive interactions to crystallize biological macromolecules, Acta Cryst. D 58 (2002) 1549–1553.
[39] Y. Wang, O. Annunziata, Comparison between protein-PEG interactions and the effect of PEG on protein-protein interactions using the liquid–liquid phase transition, J. Phys. Chem. B 111 (2007) 1222–1230.
[40] D. Kilburn, J.H. Roh, L. Guo, R.M. Briber, S.A. Woodson, Molecular crowding stabilizes folded RNA structure by the excluded volume effect, J. Am. Chem. Soc. 132 (2010) 8690–8696.
[41] J.M. Rohwer, P.W. Postma, B.N. Kholodenko, H.V. Westerhoff, Implications of macromolecular crowding for signal transduction and metabolite channeling, Proc. Natl. Acad. Sci. U.S.A. 95 (1998) 10547–10552.
[42] O. Regev, R. Zana, Aggregation behavior of tyloxapol, a nonionic surfactant oligomer, in aqueous solution, J. Colloid Interface Sci. 210 (1999) 8–17.
[43] H. Schott, Comparing the surface chemical properties and the effect of salts on the cloud point of a conventional nonionic surfactant, octoxynol 9 (Triton X-100), and of Its oligomer, tyloxapol (Triton WR-1339), J. Colloid Interface Sci. 205 (1998) 496–502.
[44] D.G. Miller, J.G. Albright, Optical methods, in: W.A. Wakeham, A. Nagashima, J.V. Sengers (Eds.), Measurement of the Transport Properties of Fluids: Experimental Thermodynamics, Vol. III, Blackwell Scientific Publications, Oxford, 1991, pp. 272–294.
[45] J.G. Albright, O. Annunziata, D.G. Miller, L. Paduano, A.J. Pearlstein, Precision measurements of binary and multicomponent diffusion coefficients in protein solutions relevant to crystal growth: lysozyme chloride in water and aqueous NaCl at pH 4.5 and 25 °C, J. Am. Chem. Soc. 121 (1999) 3256–3266.
[46] D.G. Miller, V. Vitagliano, R. Sartorio, Some comments on multicomponent diffusion: negative main term diffusion coefficients, second law constraints, solvent choices, and reference frame transformations, J. Phys. Chem. 90 (1986) 1509–1519.
[47] L.A. Woolf, D.G. Miller, L.J. Gosting, Isothermal diffusion coefficients of the H_2O–glycine–KCl system; tests of the Onsager reciprocal relations, J. Am. Chem. Soc. 84 (1962) 317–331.
[48] D.G. Miller, Ternary isothermal diffusion and the validity of the Onsager reciprocity relations, J. Phys. Chem. 63 (1958) 570–578.
[49] O. Annunziata, L. Paduano, A.J. Pearlstein, D.G. Miller, J.G. Albright, Extraction of thermodynamic data from ternary diffusion coefficients. Use of precision measurements for aqueous lysozyme chloride–NaCl at 25 °C to determine the change of lysozyme chloride chemical potential with increasing NaCl concentration well into the supersaturated region, J. Am. Chem. Soc. 122 (2000) 5916–5928.
[50] O. Annunziata, L. Paduano, A.J. Pearlstein, D.G. Miller, J.G. Albright, The effect of salt on protein chemical potential determined by ternary diffusion, J. Phys. Chem. B 110 (2006) 1405–1415.
[51] O. Annunziata, On the role of solute solvation and excluded-volume interactions in coupled diffusion, J. Phys. Chem. B 112 (2008) 11968–11975.
[52] A. Lomakin, N. Asherie, G.B. Benedek, Monte carlo study of phase separation in aqueous protein solutions, J. Chem. Phys. 104 (1996) 1646–1656.
[53] D.G. Miller, The Onsager relations; experimental evidence, in: J.J. Delgado Domingos, M.N.R. Nina, J.H. Whitelaw (Eds.), Foundations of Continuum Thermodynamics, MacMillan Press, London, 1974, pp. 185–214.
[54] L. Onsager, Reciprocal relations in irreversible processes. I, Phys. Rev. 37 (1931) 405–426.
[55] H. Zhang, O. Annunziata, Effect of macromolecular polydispersity on diffusion coefficients measured by Rayleigh interferometry, J. Phys. Chem. B 112 (2008) 3633–3643.
[56] K.S. Schmitz, An Introduction to Dynamic Light Scattering by Macromolecules, Academic Press, San Diego, 1990, pp 11–30.
[57] W. Kaye, A. Havlik, Low Angle Laser Light Scattering-Absolute Calibration, J. Appl. Opt. 12 (1973) 541-550. N. Kozer, Y.Y., Kuttner, G., Haran, G. Schreiber.
[58] N. Kozer, Y.Y. Kuttner, G. Haran, G. Schreiber, Protein–protein association in polymer solutions: from dilute to semidilute to concentrated, Biophys. J. 92 (2007) 2139–2149.
[59] H. Zhang, O. Annunziata, Modulation of drug transport properties by multicomponent diffusion in surfactant aqueous solutions, Langmuir 24 (2008) 10680–10687.
[60] J.G. Albright, L. Paduano, R. Sartorio, A. Vergara, V. Vitagliano, Multicomponent diffusion in systems containing molecules of different size. 1. Mutual diffusion in the ternary system poly(ethylene glycol) 2000 + poly(ethylene glycol) 200 + water, J. Chem. Eng. Data 46 (2001) 1283–1291.
[61] A. Einstein, Über die von der molekularkinetischen Theorie der Wärme geforderte Bewegung von in ruhenden Flüssigkeiten suspendierten Teilchen, Annalen der Physik 17 (1905) 549–560.
[62] C. Tanford, Physical Chemistry of Macromolecules, Wiley, New York, 1961, p. 356.
[63] J. Kestin, M. Sokolov, W.A. Wakeham, Viscosity of liquid water in the range −8 °C to 150 °C, J. Phys. Chem. Ref. Data 7 (1978) 941–948.
[64] S. Kirincic, C. Klofutar, Viscosity of aqueous solutions of polyethylene glycols at 298.15 K, Fluid Phase Equilibria 155 (1999) 311–325.

[65] K. Westesen, M.H.J. Koch, Phase diagram of tyloxapol and water – II, Int. J. Pharm. 103 (1994) 225–236.
[66] R. Tuinier, J.K.G. Dhont, T.-H. Fan, Motion of a sphere through a polymer solution, Phys. Rev. E 75 (2007) 011803.
[67] T.-H. Fan, J.K.G. Dhont, R. Tuinier, How depletion affects sphere motion through solutions containing macromolecules, Europhys. Lett. 75 (2006) 929–935.
[68] R.J. Bearman, On the molecular basis of some current theories of diffusion, J. Phys. Chem. 65 (1961) 1961–1968.
[69] X. Liu, A. Bardow, T.J.H. Vlugt, Multicomponent Maxwell-Stefan diffusivities at infinite dilution, Ind. Eng. Chem. Res. 50 (2011) 4776–4782.